Dust Flow Separator Type Electrostatic Precipitator for a Particulate Matter Emission Control from Natural Gas Combution

L. GUAN[1], G. HARVEL[1,2], S. PARK, J.S. CHANG[1]
(1 McIARS and Department of Engineering Physics, McMaster University, Hamilton, Ontario, Canada
2 Corresponding Author, Energy Systems and Nuclear Science, University of Ontario Institute of Technology, Ontario, Canada
E-mail: Glenn.Harvel@uoit.ca)

Abstract: Control of Particulate matter (PM) emission is a key pollution issue affecting the environment and human health, especially sizes that range below 10 μm. The objective of this work is to develop a dust flow separator type electrostatic precipitator (DFS-ESP) for the effective control of fine particulate matter emission from natural gas combustion. An experiment was conducted for natural gas combustion exhaust flow rates from 2.5 Nm^3/h to 9 Nm^3/h, ESP applied voltage from 0 to 30 kV, and combustion gas temperature from 80 ℃ to 160 ℃. Particle measurements were conducted at upstream, downstream and middle of the DFS-ESP system. The experimental results show that particle size emitted from the natural gas combustion ranges in 17 nm -300 nm in diameter, volume density ranges approximately from 5×10^8 #pt/m^3 to 5×10^9 #pt/m^3 depending on the combustion conditions. The dust flow separator can concentrate 90% of fine particles in 1%-3% of the gas flow and divert it to the ESP section from the main flow channel allowing a higher efficiency for particle removal. In terms of overall particle collection efficiency, the DFS-ESP system can remove up to 95% particles based on the number density.

Keywords: Electrostatic Precipitator, Flow Separation, Fine Particulate Matter, Emission Control

1 INTRODUCTION

Among all the pollutants, particulate matter (PM) contributes to more severe effects on both the environment and human health than normally realized [1]. PMs, ranging in diameter from several nanometers to a few hundred-micrometers, originate from power plants, automobile exhaust, steel manufacturing, pulp and paper plants, food processing, etc. as well as commercial buildings and home ventilation systems [1]. Particles less than 2.5 μm ($PM_{2.5}$, also named respirable particles) can penetrate deep into human lungs, deposit in the alveolus, and may be transported to systemic apparatus or tissue leading to various health problems [2]. For this reason, new regulations on PM control are expected from existing PM_{10} to the new emission limits of $PM_{2.5}$.

Particle control technologies have been developed and commercialized for centuries. There are five major approaches[3] for removing PMs based on different mechanisms: (1) settling and momentum separators by gravity, inertia and centrifugal effects such as cyclones, baffle chambers and settling chambers; (2) filtration separators by diffusion, interception, such as fabric filters, paper filters and baghouse filter; (3) wet collectors mainly scrubbers by impingement, diffusion, thermal gradients and electrostatic attraction; (4) acoustic separators by agglomeration resulting from sound waves; (5) electrostatic precipitation by electrostatic forces.

The electrostatic precipitator (ESP) is the most effective equipment for removing submicron (D_p<1 μm) and even ultrafine particles (D_p<0.1 μm) as small as 0.01 μm, plus ESPs have very high collection efficiency for almost all size ranges of particles, low pressure drop, lower operation cost, and ease of maintenance[3,4]. Typical types of existing ESP can be classified as wire-plate and wire-tube ESP. In this work, the wire-tube type ESP is utilized.

This research focuses on the control of submicron and ultrafine particles from natural gas combustion exhaust. Natural gas is an increasingly important source of energy and has been considered as a cleaner source, since the main pollutants from the combustion of natural gas (CO_2, CO, NO_x, and hydrocarbons) are relatively lower than for other fossil fuels, e.g. coal and oil, and PMs are relatively small in terms of mass fraction (mg/m^3). However, recent studies show that a significant number of ultrafine particles are observed from natural gas combustion exhaust, size range below 0.1 μm [5], which may be hazardous to human health. Therefore, characterization of the PM emission from natural gas combustion is an important research objective.

The conventional ESPs have several limitations. Firstly, the particle size collection efficiency in terms of number density for the ultrafine- or submicron-particles by a conventional ESP is relatively low, since these particles are mostly small in mass loading but very large in number density [6-11]. Secondly, heavy dust loading could cause corona quenching of the discharge electrode and a highly possible locally rise electric field in the region near the collecting electrode to trigger sparking [11, 12]. Thirdly, the particle re-entrainment problem could be generated during the rapping process, or back corona [13-15]. Therefore, the dust flow separator type electrostatic precipitator (DFS-ESP) is proposed to solve these problems in PM control from natural gas combustion exhaust.

2 EXPERIMENTAL APPARATUS

Fig.1 shows the schematic of the experiment loop. There are three sampling ports, MP1, MP2 and MP3, upstream, downstream, and in the middle of the main branch of the dust flow separator type electrostatic precipitator (DFS-ESP). The sample ports are made for particulate matter sampling, pressure and temperature monitoring, and flow profile detection in the main branch and ESP branch under different test conditions. There is a small heat exchanger located directly before the particle sampling instruments, to eliminate most of the condensate in the sample stream, to ensure the instruments are working properly. Heat exchanger is placed at upstream of DFS-ESP, for the purpose of temperature control; and hot air line is injected at the inlet of DFS-ESP, for the purpose of dilution.

The total flow rate in the loop ranged from 2.5 Nm^3/h-9 Nm^3/h. The temperature of the flue gas at the exhaust line varied from 160 ℃ at measuring port 1 (MP1) to 80 ℃ at measuring port 2 (MP2). The particulate matter created during natural gas combustion has been sampled from various locations within a loop and characterized by using Environmental Electron Scanning Microscopy (ESEM), where after particle sampling, Condensation Nucleation Particle Counter (CNPC—TSI), and optical particle counter (OPC—HazDust III) are on-line as shown in Fig.1.

Schematic configuration of the dust flow separator type electrostatic precipitator (DFS-ESP) used in this experiment is shown in Fig. 2. The basic structure of the DFS-ESP consists of a main run section of Pyrex glass sleeve tubes (O.D. 90 mm, I.D. 76 mm and 254 mm long), with a Stainless Steel pipe (I.D. 63.5 mm and 760 mm long) as the flow separator. The flow separator diverts flow into a branch run containing the ESP which then rejoins the main run flow at the end of the stainless steel pipe insert. An Aluminium pipe (I.D.63.5 mm and 430 mm long) in the ESP branch is used as the collection electrode of the wire-pipe ESP and a 0.7 mm diameter wire is used as the discharge electrode.

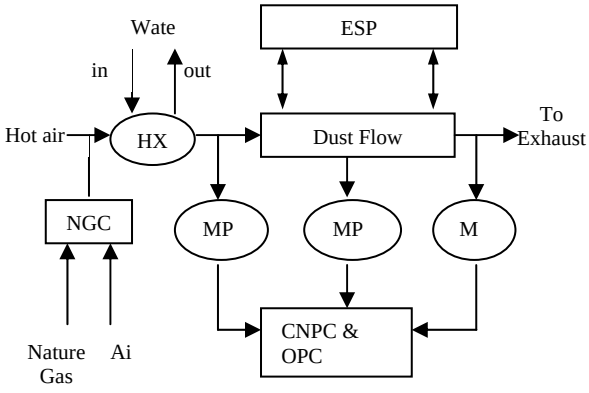

Fig. 1 Schematic of experimental loop

NGC- Natural Gas Combustor, HX – Heat Exchanger, MP – Sampling ports for PM, temperature, and pressure, ESP – Electrostatic Precipitator, CNPC – Condensation Nucleation Particle Counter, OPC – Optical Particle Counter

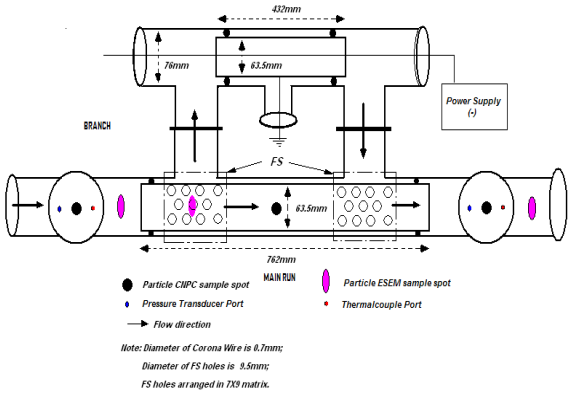

Fig. 2 Schematic of DFS-ESP

3 EXPERIMENTAL RESULTS

3.1 Particles Characteristic

ESEM images were taken of deposited particles sampled from center of flow dusts at upstream (MP1), downstream (MP2) of DFS-ESP, and the upstream flow separator wall. Fig. 3 shows a typical example of these images, where the corresponding size distribution analysis is shown in Fig. 4. The ESEM images indicated that the majority of the deposited fine particles are agglomerated structures of the near spherical shape. The size distribution determined by ESEM image analysis shows that particles sampled from three locations have the similar size distribution and particle sizes from 50 to 100 nm. The mean particle diameter is estimated approximately 84 nm, 96 nm and 85 nm for locations MP1, MP2 and the upstream flow separator wall respectively.

Fig. 3 Typical ESEM image of deposited particles Sampled from tube center at MP1

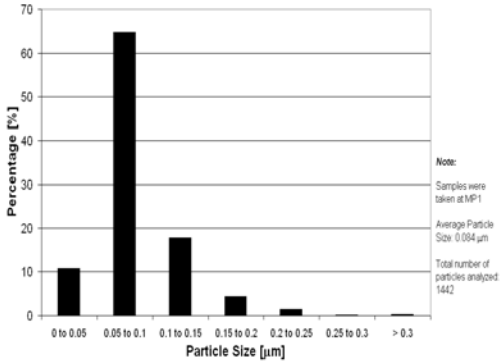

Fig. 4 Size distribution of deposited particles from tube center at MP1 for Q=7Nm^3/h, T=160℃

Particle size distributions at different locations analyzed by CNPC method are also analyzed. The size distribution determined by CNPC method has a bimodal distribution with peaks for particle groups in the range from 17 nm to 41 nm and 132 nm to 162 nm in diameter, at MP1; and the size distribution at MP3 shows a similar bimodal distribution with the peaks for particle groups in the range from 41 nm to 72 nm and greater than 162 nm. The total particle number density varies with the combustion situation (sufficient combustion/ insufficient combustion), approximately ranging from 5×10^8 #pt/m^3 to 5×10^9 #pt/m^3, taking into account changes in inlet air flow rate, exhaust temperature, and pressure drop across the system.

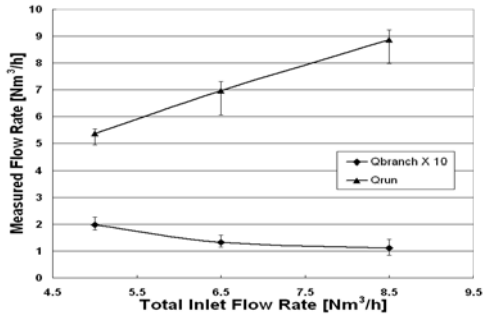

Fig. 5 Flow rate at branch and run channel vs. total inlet gas flow rate

3.2 Characteristic of Dust Flow Separator

The role of the dust flow separator is to separate most of the fine particles from the exhaust flow to ESP branch, while maintaining most of the flow in the main stream. Hence, characterizing the flow separation, particle separation and pressure drop of the DFS-ESP system were conducted.

3.2.1 Gas Flow Separation Characteristics

Based on the flow velocity distribution in main branch at location MP3, the flowrate was determined, where by subtracting the flow rate of the main channel (MP3) from that at upstream (MP1), the flow rate in the ESP branch is determined. The comparison for flow rates between ESP branch and mainstream (run) is shown in Fig. 10. Since the flow rate in the ESP branch is relatively small, the real value is scaled 10 times to observe the trend.

Fig. 5 shows that, the main flow increases and branch flow decreases as increasing total inlet flow rate. This demonstrates less gas flow to the ESP branch as the total inlet flow increases. Flow separation fraction in branch is determined by:

$$\eta = (Q_{\mathrm{MP1}} - Q_{\mathrm{MP3}}) / Q_{\mathrm{MP1}}$$

Therefore, for the different total inlet flows (5 Nm^3/h, 7 Nm^3/h and 8.5 Nm^3/h), the gas flow separation fraction are approximately 3%, 2% and 1% respectively, where the major gas flow is in the main flow channel and less in ESP branch.

3.2.2 Particle Separation Characteristic

The particle number density for different total inlet gas flow rate at upstream (MP1) and middle of main channel (MP3) are shown in Fig.6; and the corresponding size distribution for MP1, MP2 and MP3 at 7 Nm^3/h is shown in Fig. 7. Fig. 6 shows that the particle number density increases with increasing total inlet flow at MP1, and decreases at MP3, which demonstrates that more particles are separated to the ESP branch at higher inlet gas flow. Fig. 13 shows the particle size distribution at MP1, MP2 and MP3 for total inlet flow at 7 Nm^3/h. First of all, fine size particles (17 nm-41nm) range at MP1 (upstream) and MP2 (downstream) is approximately 15% difference, which most likely is the function of deposition of the whole DFS-ESP system. Secondly, particles with size range larger than 162 nm occupy most of the portion at MP3. Based on the above observations, the particles with smaller size range are separated at DFS section, especially effective with 17 nm to 41 nm size range; and particles show the trend of agglomeration at MP2 and MP3 at higher size range.

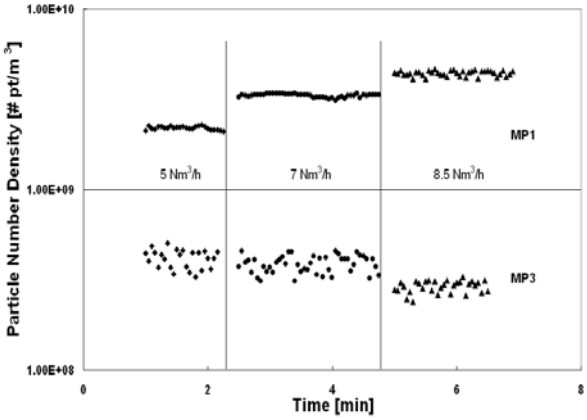

Fig. 6 Comparison of particle number density for different total inlet flow rate at MP1 and MP3

Furthermore, the separation fraction can be computed by,

$$\eta = \frac{(N_{\mathrm{MP1}} - N_{\mathrm{MP3}})}{N_{\mathrm{MP1}}} \times 100\%$$

so that, separation fraction for 17 nm-41 nm size range particles is 99.4% to the ESP branch, and overall separation fraction to the ESP branch is around 95% for all particle sizes.

3.2.3 DFS-ESP Particles Collection Efficiency

Dust particle collection efficiency based on particle density as a function of ESP applied voltage is shown in Fig. 8 for which gas flow for inlet gas temperature 165°C and dust density 2×10^9#pt/m^3-4×10^9#pt/m^3. From the flow rate analysis in previous paragraph, the ESP branch flow rates are approximately 0.2 and 0.14 Nm^3/h for 5 Nm^3/h and 7 Nm^3/h total inlet gas flow rates respectively, and these information as inputs for the MESP code [16], to compare dust particle collection efficiency as shown in Fig. 8.

Fig. 8 shows that particle collection efficiency based on

number density increases with increasing total inlet gas flow rate and ESP applied voltage, where the relatively low collection efficiency before corona-onset voltage may be due to the diffusion and thermophoresis effects within the entire system. The experimental results and MESP code prediction agree qualitatively and quantitatively for above 20kV ESP voltage and 7 Nm^3/h gas flow rate, where quantitative analysis shows that about 95% particle collection efficiency based on the number concentration can be obtained at 7 Nm^3/h and ESP voltage above 20kV.

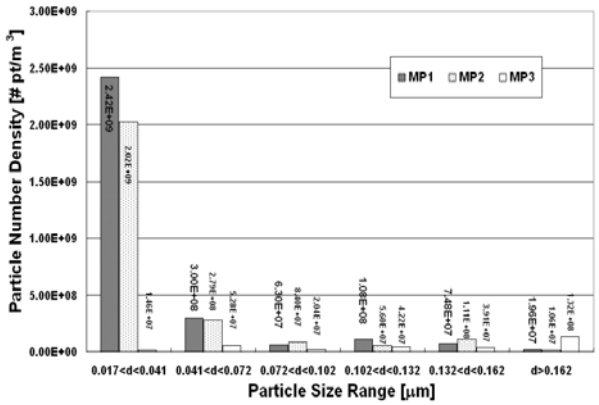

Fig. 7 Size distribution comparison for MP1, MP2 and MP3 at 7Nm^3/h and 0kV by CNPC-PSS with 30nm increment

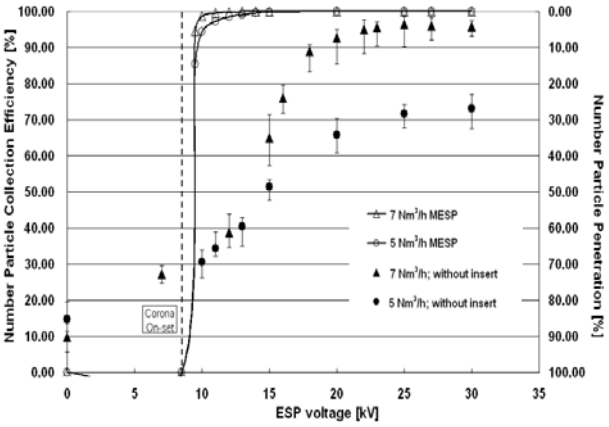

Fig. 8 Particle collection efficiency based on number density versus ESP voltage for different gas flow rates without insert, compared with MESP modeling result

The particle mass concentration based collection efficiency is presented in Fig. 9, where particle mass density is around 1.05 mg/cm^3. Comparing with the number density based particle collection efficiency, particle mass density based collection efficiency is relatively smaller, where the highest value is around 76%. This discrepancy might due to the fact that the agglomerated larger dust particles may not well separated to reach ESP branch due to the larger inertia. Note the detection limit of the instrument used for mass density ($\pm 0.01 mg/m^3$) may contain a few percentage error in the present range of measurement.

Further analysis for partial particle collection efficiency is conducted using CNPC-PSS. Results are shown in Fig. 10 and 11, for the collection efficiency at 20kV ESP voltage, and 5 Nm^3/h and 7 Nm^3/h gas flow rate, respectively. It indicates that the most particle number collection efficiency can be obtained for fine particles in the range of 17 nm to 41 nm, which is 86.6% for 5 Nm^3/h gas flow rate, and 95.6% for 7 Nm^3/h gas flow rate. Agglomeration of particle can also be observed for particles' size in the ranges of 72 to 102 nm and above 162 nm.

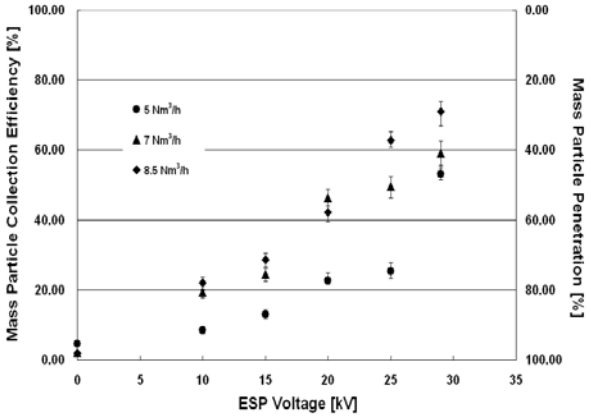

Fig. 9 Particle collection efficiency based on mass fraction versus ESP voltage for different gas flow rates without insert

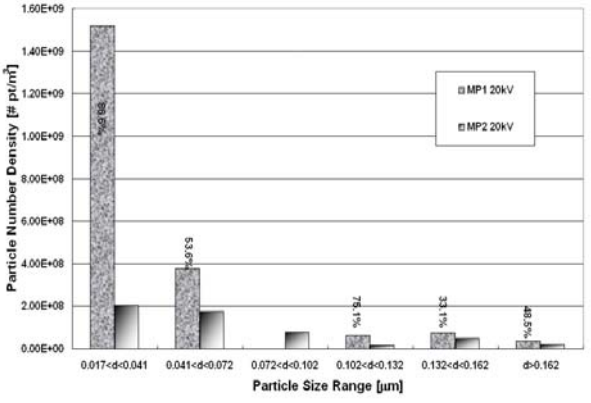

Fig. 10 Particle collection efficiency based on number density at 20kV ESP voltage and 5 Nm^3/h by CNPC-PSS with 30 nm increment

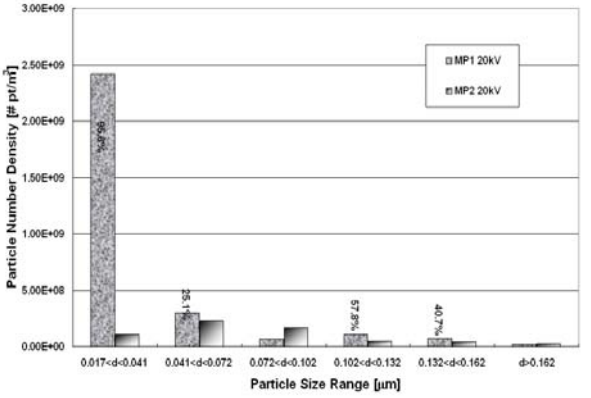

Fig. 11 Particle collection efficiency based on number density at 20 kV ESP voltage and 7 Nm^3/h by CNPC-PSS with 30 nm increment

4 CONCLUSIONS

Dust flow separator type electrostatic precipitator for a control of fine particle emission from natural gas combustion was experimentally and numerically investigated, and the following conclusions were obtained:

1. Size of particles from natural gas combustion ranges from smaller than 17 nm to 300 nm, with a maximum particle mass density at 1.05 mg/cm^3 and number density approximately at 5×10^8 to 5×10^9 $\#pt/m^3$ depending on combustion conditions.
2. Particle size shows a bimodal distribution with maximum density for particle size groups in the range from 17 nm to 41 nm and 132 nm to 162 nm in diameter, at upstream of DFS-ESP; and the size distribution at main flow channel of DFS-ESP shows a similar bimodal distribution with the maximum for particle groups in the range from 41 nm to 72 nm and greater than 162 nm.
3. The flow separation fraction to ESP branch of the flow separator are approximately 3%, 2% and 1% for gas flow with respects to 5 Nm^3/h, 7 Nm^3/h and 8.5 Nm^3/h total inlet flow rate respectively, while the particle separation fraction to ESP branch are 97%, 98% and 99% for 5 Nm^3/h, 7 Nm^3/h and 8.5 Nm^3/h total inlet gas flow rate respectively.
4. The experimental results and MESP code prediction for particle collection efficiency based on particle number density for ESP branch agree qualitatively and quantitatively for above 20 kV ESP voltage and 7 Nm^3/h gas flow rate, where quantitative analysis shows that about 95% particle collection efficiency based on the number concentration can be obtained.
5. The collection efficiency based on particle mass density increases with increasing ESP voltage and total inlet gas flow. However, compared with those based on particle number density, the collection efficiency is lower with a maximum achievable value of 76% for 8.5 Nm^3/h inlet flow and 30 kV ESP voltage.

ACKNOWLEDGEMENTS

The authors wish to thank D. Borocilo, K. Urashima, J. Hoard, D. Ewing, and C. Ching for their valuable discussions and comments.

REFERENCES

1. Jacobson, M.Z. Aerosol particles in smog and the global environment, Atmospheric pollution: History, science, and regulation, Cambridge University Press, 116-143, 2002.
2. Task group on lung dynamics, Health Physics, Vol. 12, 173, 1966.
3. Marchello, J.M. Particle control equipment, Control of air pollution sources, New York: Marcel Dekker, Inc., 119-184, 1976.
4. Masuda, S. and Hosokawa, Electrostatic precipitation, Handbook of electrostatic processes, Editors: J.S.Chang, A.J.Kelly, and J.M.Crowley, Marcel Dekker, Inc., New York, Ch.21, 441-479, 1995.
5. Brocilo, D., Guan, L., Harvel, G.D., and Chang, J.S. Characterization of particle emission from nature gas combustion, J. Aerosol Science, Volume II, 877-878, 2004.
6. Ito, T., Kubota, T., Zukeran, A., Takashi, T., Shinkai, K., Miyamoto, M., and Yoshimochi, T. Collection characteristics of submicron particles on electrostatic precipitator, J. Inst. Elect. Install, Eng. Japan, Vol. 15 (2): 113-120, 1995.
7. Zukerman, A., Looy, P.C., Chakrabarti, A., Berezin, A.A., Jayaram, S., Cross, J.D., Ito, T., and Chang, J.S. Collection Efficiency of Ultrafine Particles by ESP under sc and pulsed operating modes. IEEE Transactions of Industrial Applications, Vol. 35, 1184- 1191, 1999.
8. Riehle, C. and Loffler, F. The Effective Migration Rate in Electrostatic Precipitator, Aerosol Science Technology, Vol. 16 (12): 1288-1296, 1996.
9. Raphael, M., Rohani, S., and Soslski, F. Isoelectric precipitation of sunflower protein in a tubular precipitator. Can. J. Chem. Eng., Vol. 73, 470-483, 1995.
10. Chang, J.S., Thompson, H., Looy, P.C., Berezin, A.A., Zukeran, A., Ito, T., Jayaram, S. and Cross, J.D., Control of trace elements in combustion flue gas by a corona discharge activated conditioning agent and electrostatic precipitators, Proceedings of the 6th International conference on Electrostatic Precipitators, I.Berta, Ed. Budapest, Hungary: Tech. Univ. Budapest Press, 2-7, 1997.
11. Zukeran, A., Chang, J.S., Berezin, A.A., and Ito, T. Control of ultrafine particles from incense smoke by an air cleaning electrostatic precipitator, J. Aerosol Sci., Vol.28, suppl. 1, S289-S290, 1997.
12. Pauthenier, M.M., and Moreau-Hanot, M. Le charge des particules spheriques dans un champ ionise, J. Phys. Radium (Paris), Vol. 3, 590, 1932.
13. Mizuno, A, Electrostatic Precipitation, IEEE Transactions on Dielectrics and Electrical Insulation, Vol. 7, 615-624, 2000.
14. Masuda, S. and Mizuno, A. Flashover measurement of back discharge, J. Electrostatics, Vol. 4, pp. 215, 1978.
15. Masuda, S. Resistivity and back corona, Proceedings of International Conference on Electrostatic Precipitation, California: Monterey, 131-161, 1981.
16. Brocilo, D., Chang, J.S. and Findlay, R.D. Modeling of electrode geometry effects on dust collection efficiency of wire-plate electrostatic precipitators, Proceedings of 8th International Conference on Electrostatic Precipitation, Vol. 1, 1-18, 2001.